CHAPTER V
RESULTS AND DISCUSSION

Using Equations (3.13), (3.14), and (3.20) to investigate meniscus shapes in a system of water-air-glass at 25°C where density, ρ = 1000 kg/m^3, σ = 71.4 mN/m, and the contact angle is 10° by imposing that $\lambda = (\kappa R + R)/2$. While maintaining the annular gap width at 0.02 mm, the radii of the inner and the outer tube were varied. The results (Figures 5.1, 5.2, and 5.3) show that meniscus configurations are the same no matter how big or small the annular tube is as long as its gap width is constant. Comparing the values of meniscus heights at r = 0.985, 0.99, and 0.995 mm, three sizes of annular tubes have exactly the same height values, 0.0213, 0.0284, and 0.0213 mm, respectively.

Meniscus shapes resulted from different annular gap widths are shown in Figure 5.4. It appears that the meniscus changes with the gap width. Noting that Equation (3.20) does not contain any term of κ, so it must be corrected in order to account for κ when κ is not constant by setting H(r) = 0 at r = κR to Equation (3.19). It is observed that the analytical model solved from H(r = κR) = 0 and H(r = λR) = 0 gives nearly the same shape as shown in Figure 5.5.

The results demonstrated in Figures 5.1-5.4 show that the values of h at r = κR and R are the same due to the assumption of symmetry. However, different phenomena can be observed when λ is not fixed at the middle of the gap width (Figure 5.6). Since this study is based on the annular tube size of R = 10 mm, to satisfy the boundary conditions as shown in Figure 3.2(b), λ must be 0.99R. With λ is close to the inner wall, λ = 0.985R, the menisci is more concave than λ at the center. With λ is close to the outer wall, λ = 0.995R, the menisci is less concave than λ at the center. It is obviously due to the deviation of the boundary conditions. With the change of λ, the tip position of the meniscus changes to the assigned value and the H value changes as λ changes.

Effect of the variation of the annular gap width on the meniscus shape has already been discussed above as well as the change in the annular tube size but not

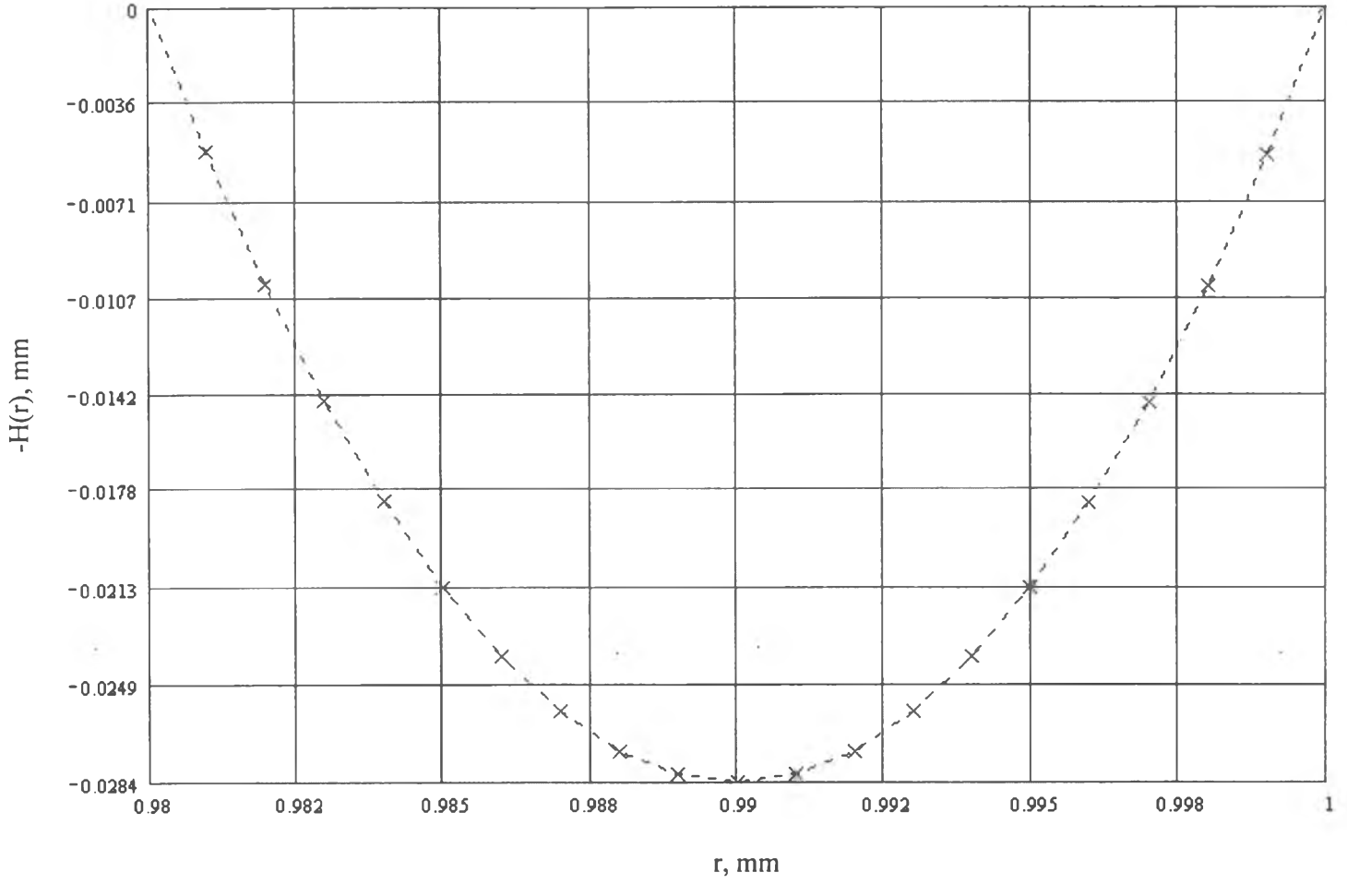

Figure 5.1 Shape of a meniscus from the analytical solution in the annulus of R = 1 mm, $\kappa = 0.98$, and $\lambda = 0.99$.

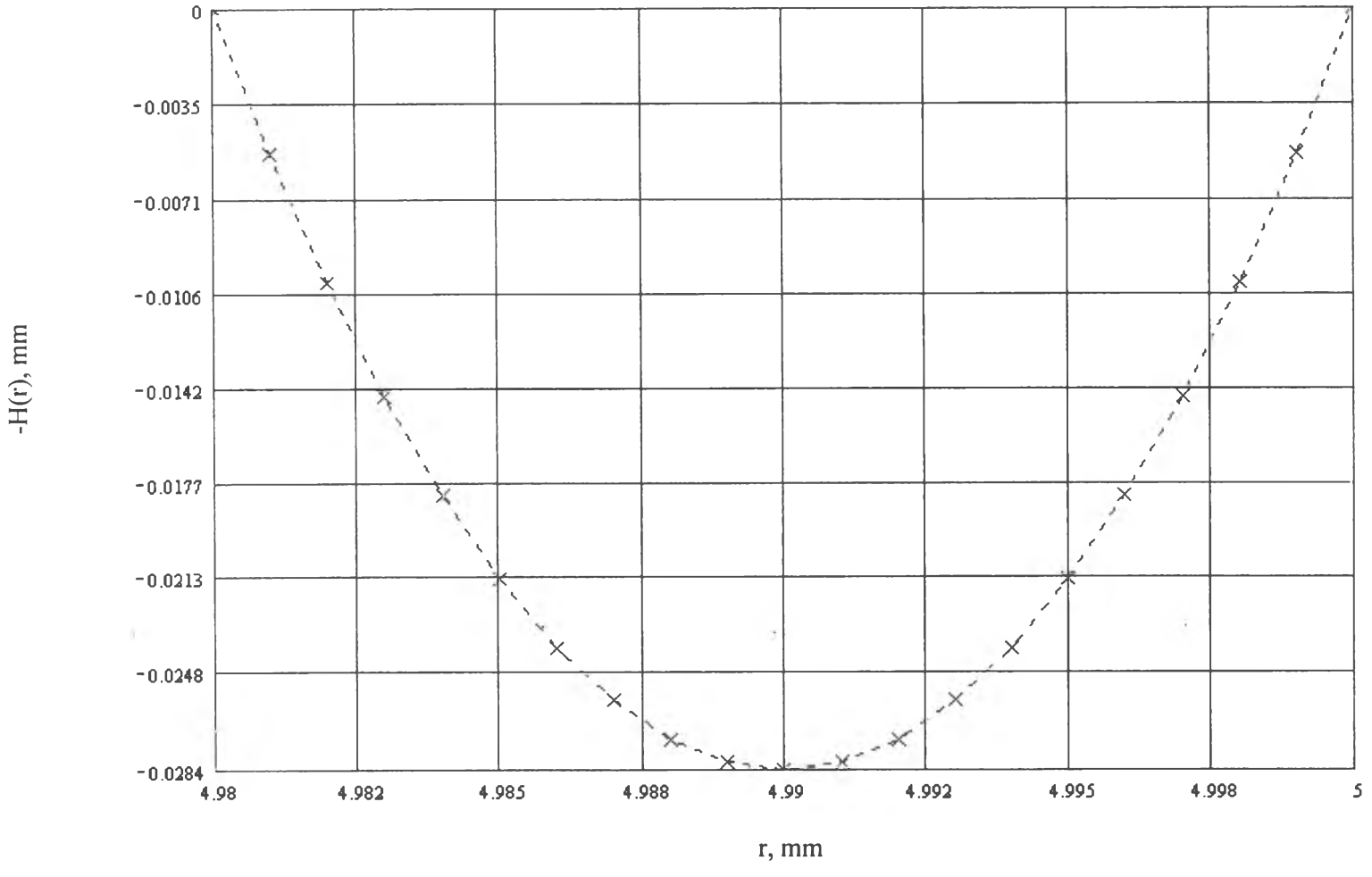

Figure 5.2 Shape of a meniscus from the analytical solution in the annulus of R = 5 mm, $\kappa = 4.98/5$, and $\lambda = 4.99/5$.

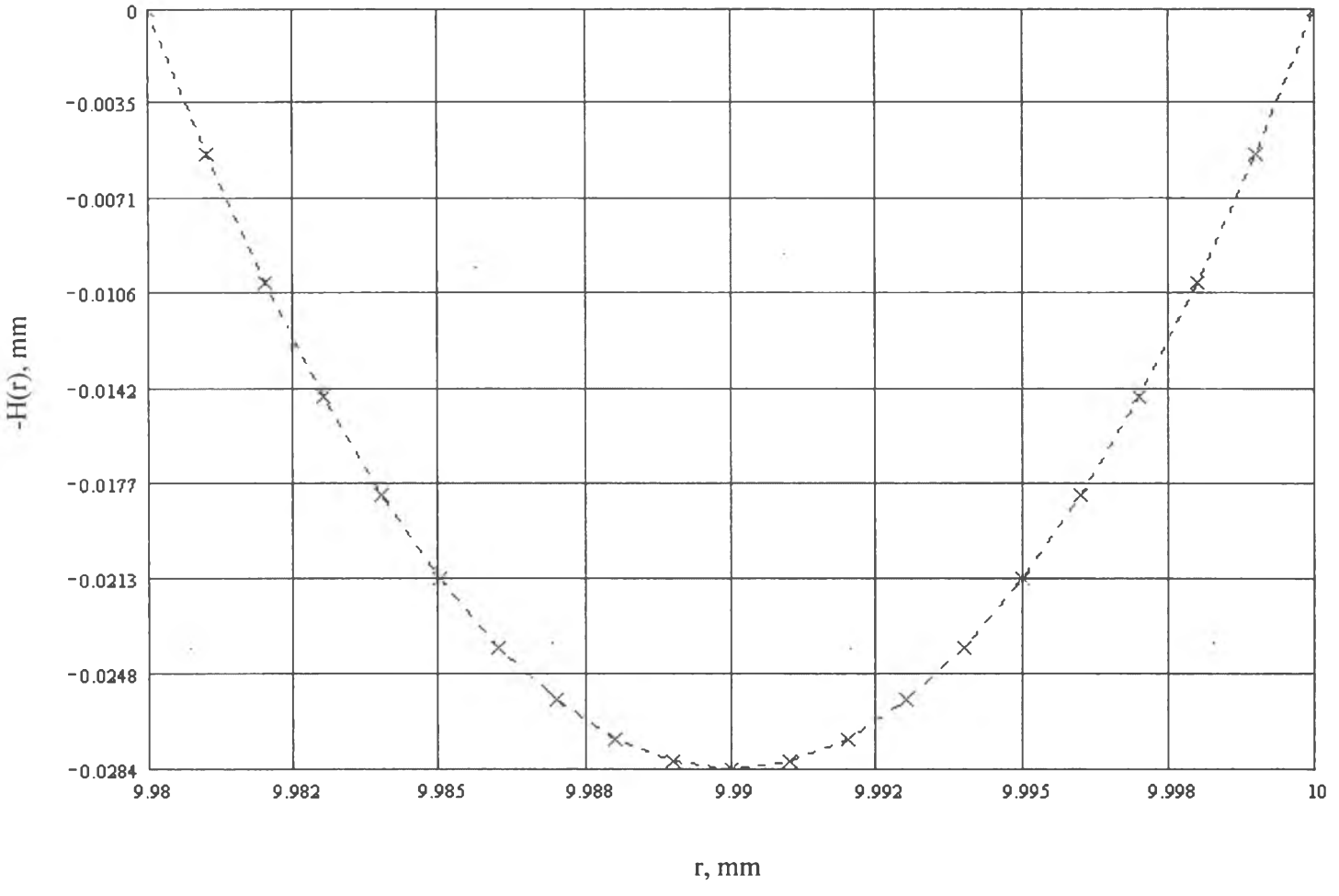

Figure 5.3 Shape of a meniscus from the analytical solution in the annulus of R = 10 mm, $\kappa = 0.98$, and $\lambda = 0.99$.

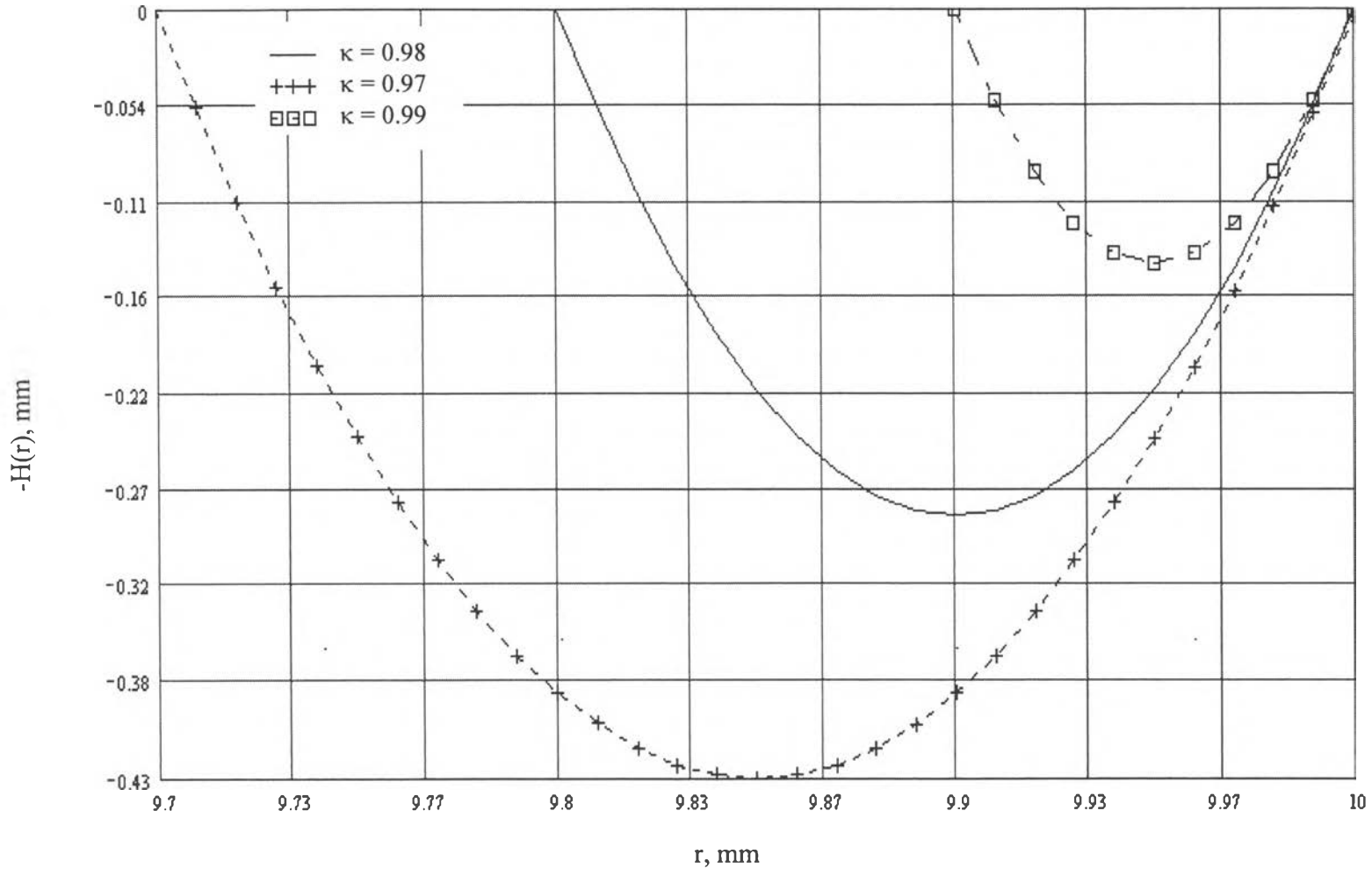

Figure 5.4 Shapes of menisci from the analytical solution with various gap widths with a constant outer tube radius, R, of 10 mm.

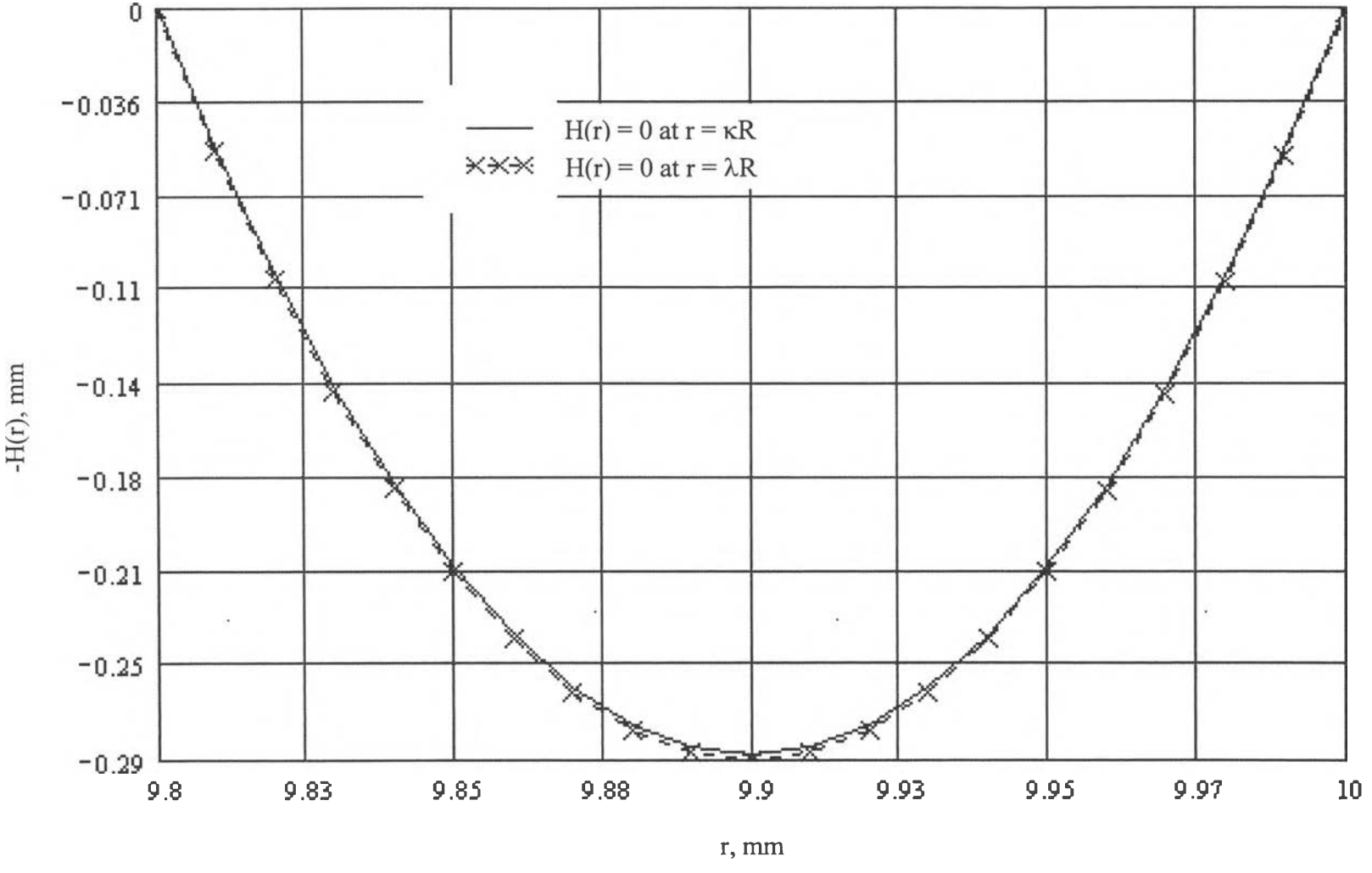

Figure 5.5 Shapes of menisci in the annulus comparing between H_0 solved analytically by setting $H(r) = 0$ at $r = \kappa R$ and $r = R$.

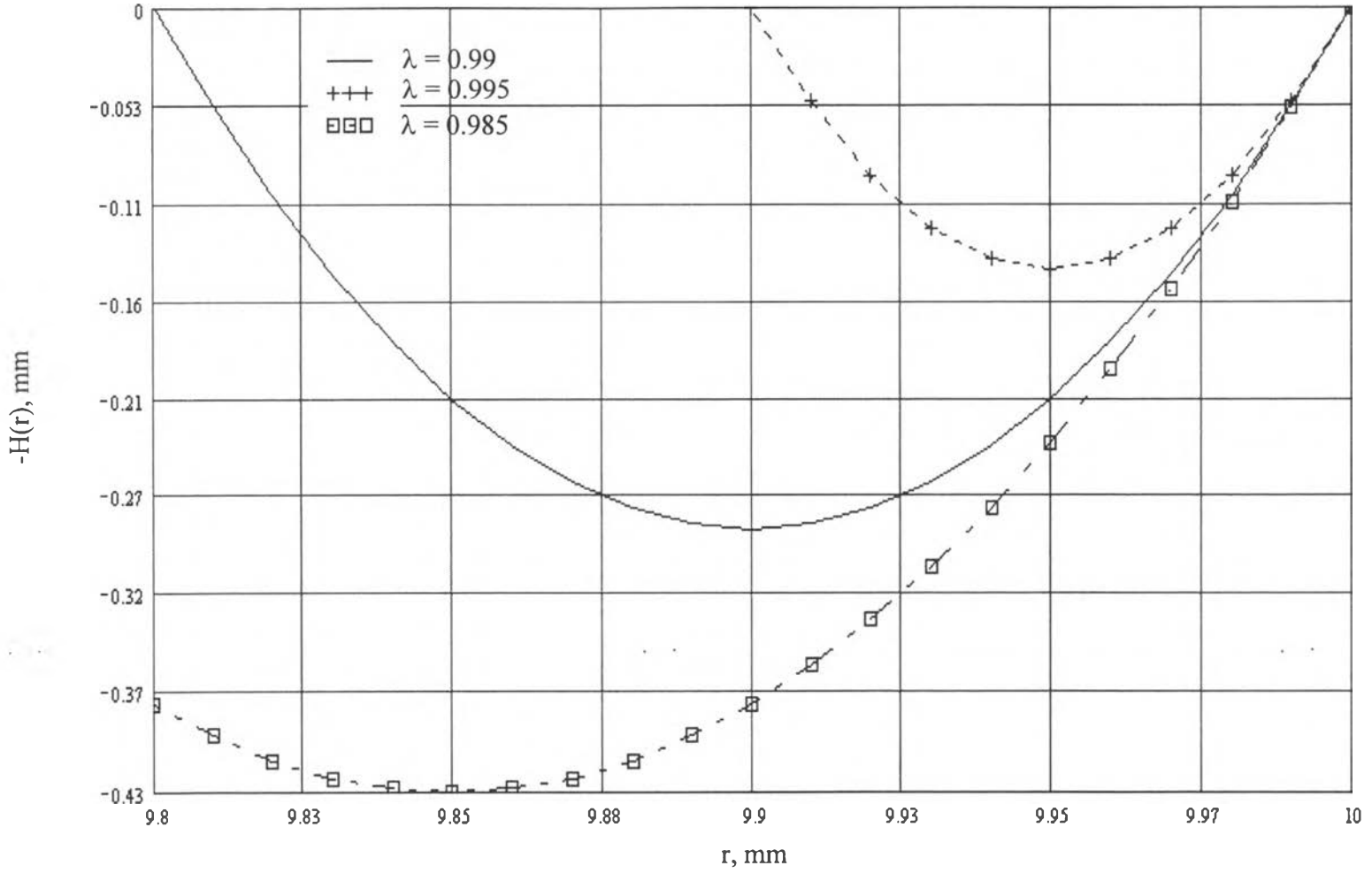

Figure 5.6 Shapes of menisci in the annulus with various positions of a meniscus tip with a constant outer tube radius, R, of 10 mm.

yet the contact angle between the fluids and the tube. The contact angle depends strongly on a surface type as shown in Table 5.1 and others (Kwok *et al.*, 1996 and Rosen, 1989). Contact angles (θ) in the table were determined from two methods, direct measurements of the contact angles and thin layer wicking. Figure 5.7 shows meniscus shapes for the water-air system at 20°C using data from Table 5.1 with the annular dimensions fixed at R = 1 mm, $\kappa = 0.98R$ and the tip of the meniscus was at the middle of the gap width, i.e. $\lambda = 0.99R$.

The curves show that ground calcite, ground glass and dolomite have more or less the same meniscus shapes but are significantly different from calcite and glass slide. The meniscus shapes of the former group and ground dolomite are nearly flat showing that the surfaces are highly hydrophobic. In contrast to the latter group, the curves are deeply concave downward indicating that the surfaces are less hydrophobic (higher hydrophilicity).

Table 5.1. Contact angles of water for various solids as determined from directed contact angle measurements (CA) and from thin layer wicking (TW) (Chibowski and Perea-Carpio, 2002)

Solid	Method	θ (°)
Calcite	CA	6.2
Ground calcite	TW	55.9
Glass slide	CA	9.0
Ground glass	TW	49.4
Dolomite	CA	51.7
Ground dolomite	TW	76.5

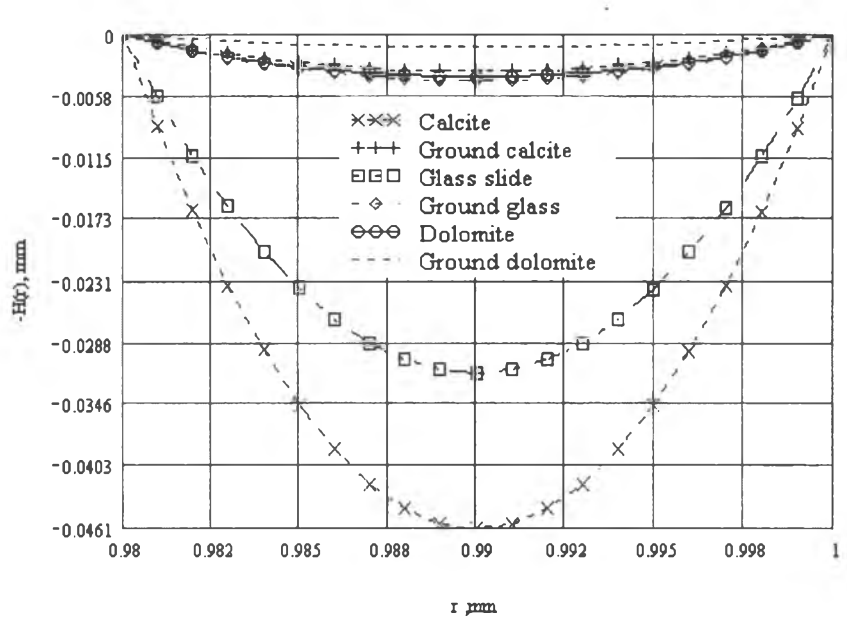

Figure 5.7 Menisci for the water-air system at 20°C. (The contact angle might not appear to be exact to values in Table 1 because the perpendicular axis is expanded relatively to the horizontal axis.)

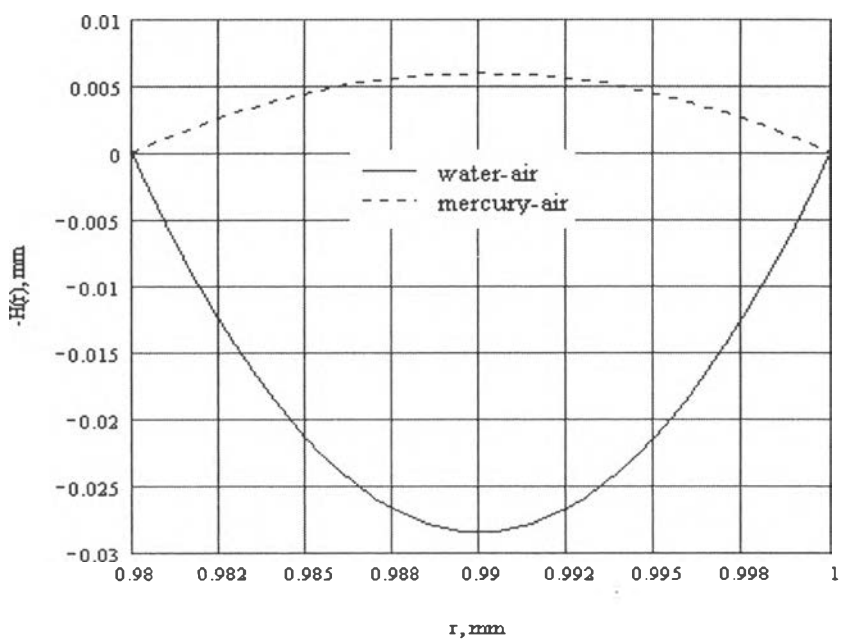

Figure 5.8 Menisci of different liquids. Contact angles: water-air = 10° (Middleman, 1998), mercury-air = 140° (Fox and Macdonald, 1994)

Figure 5.8 shows menisci for the systems of water-air and mercury-air at 20°C. According to the figure, the meniscus shapes of the two fluids are obviously opposite. That is the meniscus of water-air system is concave downward but that of mercury-air system is concave upward, corresponding to the hydrophilicity or hydrophobicity of both liquids.

The analytical model, Equation (3.20), was developed based on the assumption of an axisymmetry surface. The surface shape is independent of the angular direction. Moreover, the boundary conditions, as shown in Figure 3.2, were determined by setting the meniscus height at the inner tube wall and outer tube wall identical. From experimental results (Figure 5.9), meniscus heights at the inner and outer tube walls are apparently not identical. Contact angles at the outer tube wall of both sides are not the same, 22.9° at the right hand side (RHS) and 12.2° at the other side (LHS). So the analytical model does not satisfy with the experimental results. One reason may be that the meniscus shapes deviated from the axisymmetric surface, which is resulted from the different of the annular gap widths on both sides, 0.38 unit (LHS) and 0.40 unit (RHS). The difference in the meniscus height and contact angle between the RHS and LHS may be resulted from the fact that the annular tube was welded at one side of the tube. Heat conducted unequally throughout the tube may causes a non-homogeneous property of the glass. Reproducibility of the experiment can be achieved as shown in Figure 5.10.

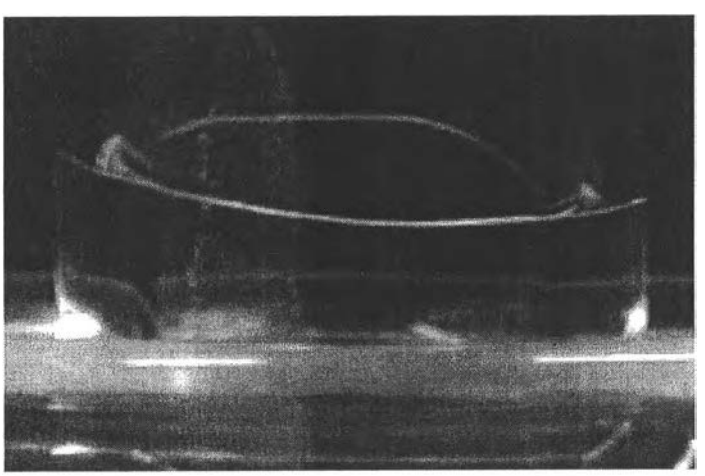

Figure 5.9 Shape of a meniscus resulted from the experiment.

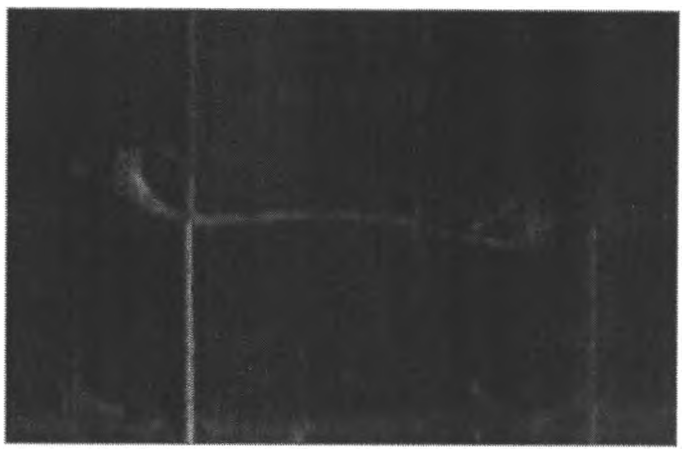

(a)

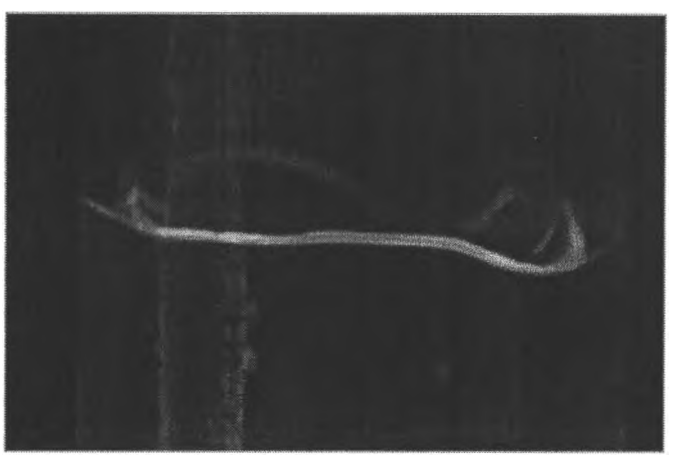

(b)

Figure 5.10 Shapes of menisci resulted from the experiments (a and b) showing that the experiments are reproducible.

The fourth-order Runge Kutta and Euler's methods were employed with a step size of 0.002 to solve Equation (3.21). The numerical solutions, in which the assumption of identical heights of the two annular tube walls was not imposed, was simulated to predict the shape of the meniscus using data from the experimental conditions and annular tube size.

Comparisons between shapes of menisci resulted from the experiments and numerical solutions are shown in Figure 5.11. The figure shows that the lines of modeling data are close to that of the experimental data, especially for the meniscus in the right hand side, where the contact angle is 12.2°. The fourth-order Runge Kutta method gives an average error of 5.37% for the LHS and 0.35% for the RHS. The Euler's method gives an average error 3.00% for the LHS and 1.47% for the RHS.

Heights of capillary rise in the annular tube resulted from the experiments are 16.14 mm at the LHS, and 14.32 at the RHS. According to Equation (3.22), the height of capillary rise is 18.2 mm. So, the discrepancies are 11.32% and 21.32%, respectively.

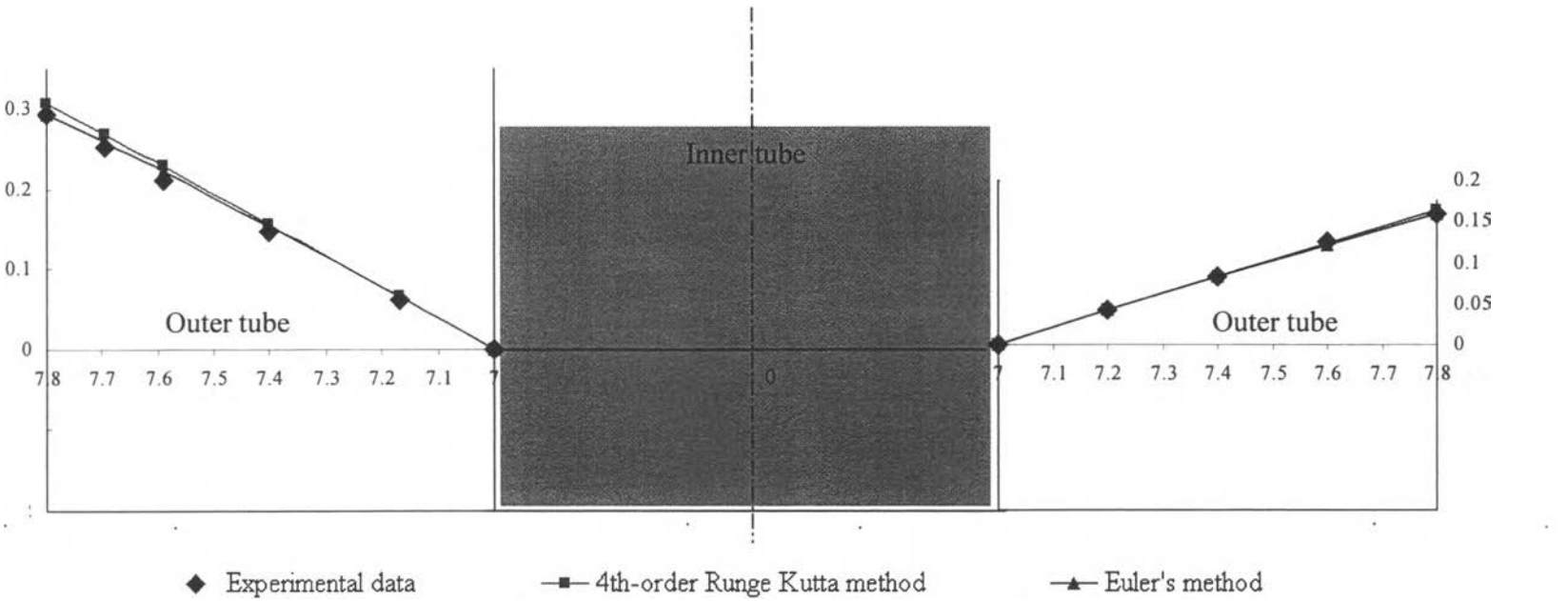

Figure 5.11 Comparison between experimental and simulation results of a contact angle of 12.2° at the RHS, and 22.9° at the LHS.